



CHALMERS
UNIVERSITY OF TECHNOLOGY

Mass transport during coagulation of cellulose-ionic liquid solutions in different non-solvents

Downloaded from: <https://research.chalmers.se>, 2023-05-05 07:25 UTC

Citation for the original published paper (version of record):

Hedlund, A., Theliander, H., Köhnke, T. (2019). Mass transport during coagulation of cellulose-ionic liquid solutions in different non-solvents. *Cellulose*, 26(16): 8525-8541.
<http://dx.doi.org/10.1007/s10570-019-02649-w>

N.B. When citing this work, cite the original published paper.



Mass transport during coagulation of cellulose-ionic liquid solutions in different non-solvents

Artur Hedlund · Hans Theliander · Tobias Köhnke

Received: 1 February 2019 / Accepted: 25 July 2019 / Published online: 19 August 2019
© The Author(s) 2019

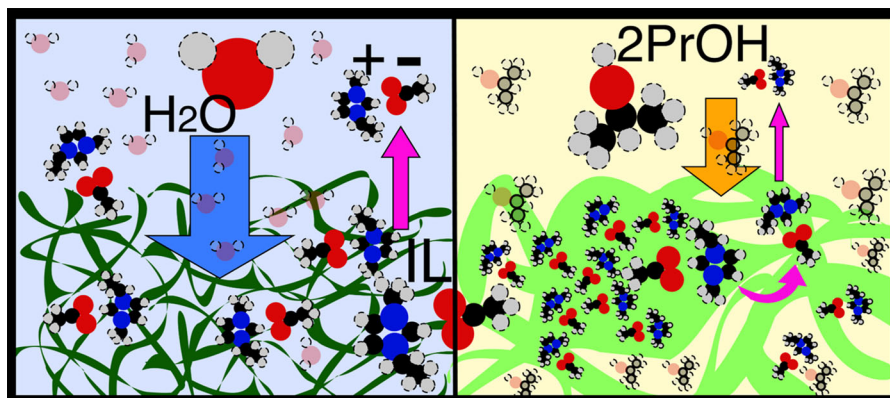
Abstract Cellulose can be regenerated from cellulose-ionic liquid (IL) solutions by immersion in water or alcohols. These compounds are potent non-solvents due to their proton-donating ability in hydrogen bonds to IL anions. Although they share this fundamental way of reducing IL solvent quality, coagulation in water is distinctly different from coagulation in alcohols with regard to the microstructures formed and the mechanisms that generate the microstructures. In this study, the possibility of mass-transport effects on microstructures was investigated. The mass-transport of all components: non-solvent (EtOH, 2PrOH), IL ([C2mim][OAc]), and a co-solvent (DMSO), during coagulation was studied. The data was compared to previous data with water as the non-solvent. Results showed that diffusion is essentially limited to a

continuous non-solvent-rich phase that is formed during phase separation in all non-solvents. There were also significant differences between non-solvents. For instance, [C2mim][OAc] diffusion coefficients were 6–9 times smaller in 2PrOH than in water, and there were apparent effects from cellulose concentration in 2PrOH that were not observed in water. The differences stem from the interactions between solvent, non-solvents, and cellulose, which can be both mutual and competitive. Weaker [C2mim][OAc]-non-solvent interactions with alcohols give more persistent [C2mim][OAc]-cellulose interactions than with water as the non-solvent, which has consequences for mass-transport.

A. Hedlund (✉) · T. Köhnke
Biobased Fibers, RISE IVF AB, Argongatan 30,
43153 Mölndal, Sweden
e-mail: artur.hedlund@ri.se

A. Hedlund · H. Theliander
Forest Products and Chemical Engineering, Chalmers
University of Technology, Gothenburg, Sweden

Graphic abstract



Keywords Cellulose · Mass transport · Coagulation · Precipitation · Ionic liquids · Non-solvent · Water · Alcohol

Introduction

Cellulose extracted from trees or other plants can be reshaped into foams, films, or fibers using dissolution–precipitation processes. Ionic liquids, ILs, constitute a new class of cellulose solvents that could provide an alternative to the viscose and NMMO technologies for such processes (Swatloski et al. 2002). ILs are organic salts with melting points below 100 °C. The anions of the salt, typically acetate or Cl^- , break up hydrogen bonds between cellulose polymers by hydrogen bonding to the cellulose hydroxyl groups (Hauru et al. 2012; Parviainen et al. 2013; Remsing et al. 2006; Zhang et al. 2010). ILs can also be mixed with polar aprotic co-solvents, such as dimethylsulfoxide (DMSO), without loss in solvent potency, i.e. in terms of moles of IL per mole of anhydroglucose units required for dissolution (Hedlund et al. 2015; Olsson et al. 2014). IL-cellulose solutions, with or without a co-solvent, can be coagulated in protic non-solvents, such as water or alcohols (Bengtsson et al. 2017; Gupta et al. 2013). However, it has been found that the resulting material properties can vary significantly depending on the non-solvent used as well as on the co-solvent content and the cellulose concentration (Wawro et al. 2014; Östlund et al. 2013). In a number of previous articles, we have reported on the coagulation of cellulose from one commonly investigated IL

cellulose solvent, 1-ethyl-3-methyl-imidazoium acetate, $[\text{C2mim}][\text{OAc}]$, and mixtures with DMSO. In the first study, the coagulation values, CVs, i.e. the necessary amounts of the non-solvents, water, EtOH, or 2PrOH, required to induce coagulation were determined (Hedlund et al. 2015). In terms of weight non-solvent per weight cellulose solution, the CVs were found to decrease with increasing cellulose concentrations (5–25 wt% cellulose) and with the choice of non-solvent in the order: 2PrOH (38–8 wt%) > EtOH (36–8 wt%) > water (26–5 wt%). The addition of DMSO as a co-solvent was also tested and was found to reduce CVs, particularly for the alcohols. In the second article (Hedlund et al. 2017), the mass-transport of non-solvent, co-solvent, and $[\text{C2mim}][\text{OAc}]$ during the coagulation of a solution membrane in water, and coagulation rates, were studied. Within that work, novel experimental methodology for the study of mass-transport in coagulating dopes was developed. The main conclusion from that study was that mass-transport accelerates in the phase-separated material because cellulose aggregates into local solid domains. From these domains, its inhibitive effect on diffusion through the surrounding liquid phase is very limited. It was also found that coagulation processes involve two stages. The first stage is coagulation, during which significantly more non-solvent is absorbed than $[\text{C2mim}][\text{OAc}]$ is emitted. The second stage was termed washout, during which the remaining $[\text{C2mim}][\text{OAc}]$ in the already coagulated material is exchanged with non-solvent. Prior to our study, there were several examples of measurements of mass transport during coagulation of cellulose solutions in

water with both N-methylmorpholin-N-oxide, NMMO (Biganska and Navard 2005; Gavillon and Budtova 2007), and in ILs (Hauru et al. 2016; Sescousse et al. 2011). However, none of these measured the mass transport of the non-solvent, which is actually the active compound that induces coagulation. In a few of these studies, the non-solvent diffusion was measured indirectly by observing the coagulation front (Biganska and Navard 2005; Hauru et al. 2016), but that method is inherently inaccurate and will overestimate the apparent diffusion coefficient by ~ 4 times (Hedlund et al. 2017).

In a recent study (Hedlund et al. 2019), we investigated coagulated materials that had been solvent-exchanged before drying to preserve the originally coagulated micro-structures. WAXS spectra and N_2 -BET specific surface area measurements were complemented with SEM images in the paper. There were significant microstructural differences between materials coagulated in water and in 2PrOH. Very low crystalline order, lesser specific surface areas and larger pores were found in 2PrOH-coagulated material.

In the present paper, the methodology for mass transport and coagulation rate measurements from the previous paper (Hedlund et al. 2017) is reapplied with two alcohols, EtOH and 2PrOH, as the non-solvents in order to compare them to water. In addition, we enquire whether the different microstructures found for cellulose materials coagulated in water or in 2PrOH (Hedlund et al. 2019) can be attributed to differences in mass-transport, as suggested by the recurring concept of hard and soft coagulation, see e.g. (Fink et al. 2001).

Materials and methods

Materials

[C2mim][OAc] of purity $> 90\%$, produced by BASF, was purchased from Sigma Aldrich. The moisture content was determined to be 0.5% with Karl-Fischer titration. Anhydrous DMSO with molecular sieve beads was also purchased from Sigma Aldrich. The cellulose used was Microcrystalline cellulose (MCC) PH-101 with $M_w = 28.4$ kDa, $M_w/M_n = 2.6$. EtOH and 2PrOH > 99.5 wt% were used as the non-solvent.

Solution preparation

The solvents used were mixtures of [C2mim][OAc] and DMSO of either 99:1 or 50:50 composition ($wt_{[C2mim][OAc]}:wt_{DMSO}$). The objective of the addition of 1 wt% of DMSO to the “pure” [C2mim][OAc] solvent was to use it as a tracer that would allow comparisons between $D_{[C2mim][OAc]}$ and D_{DMSO} in each solution and between D_{DMSO} s in different solutions. The compositions of the four solutions prepared for the experiments are summarized in Table 1, which includes the designations that will be used hereinafter. The solutions were prepared by mixing solvent and MCC in a sealed overhead mixer to minimize moisture exposure, as described previously (Hedlund et al. 2017).

Mass transport measurements

A method previously described (Hedlund et al. 2017) allows for the exposure of ≈ 0.3 g of solution to ≈ 30 g of coagulation liquid in a repeatable and controlled manner, for a well-defined time, without prior exposure to the atmosphere. The method entails the coating of a steel rod with a solution layer, 0.35 mm thick, before immersion in the non-solvent. The method allows weighing the solution before and after immersion and coagulation and, thus, calculating the difference in weight per initial mass, i.e. the net mass gain, NMG.

The temperature was kept within 21° to 23° °C during the measurement. For each solution-NS-combination, 15–25 measurements were performed with residence times varied between 4 and 3×10^5 s. The requisite number of measurements was chosen based on coagulation speed and observed variability, which depends mainly on the mechanical robustness of the coagulated material.

Coagulation front propagation rate measurement

Another method, also previously described (Hedlund et al. 2017), allows for the observation of opaque coagulated material that advances through the cellulose solutions along a glass tube. The solution was exposed to the coagulant from one end of the tube. The thickness of the coagulated material was measured with a microscope at times ranging from 100 to 9000 s. The data points for the coagulation depth were

Table 1 Composition of solutions used in the study

Solution designation (wt _{[C2mim][OAc]} :wt _{DMSO} -wt%MCC)	wt% MCC	wt% [C2mim][OAc]	wt% DMSO
99:1-5%MCC	5	94.05	0.95
99:1-14.3%MCC	14.3	84.85	0.85
99:1-25%MCC	25	74.25	0.75
50:50-14.3%MCC	14.3	42.85	42.85

plotted against $t^{1/2}$, linear plots were obtained, and the slopes were evaluated. For details regarding equipment and processing of data, cf. Hedlund et al. (2017).

[C2mim][OAc] concentration with conductivity measurements

The conductivity of coagulation liquids was measured with a standard handheld device, a 470 Cond Meter from Jenway. The alcohol baths were mixed in a ratio of 1:4 with distilled water to perform measurements in aqueous solutions. The reference measurements gave power-law expressions for the concentration as a function of conductivity in the alcohol-EmimAc mixtures diluted with water: $C_{IL}[w/w] = 3.4427 * 10^{-06} * Cond.[\mu S]^{1.067}$ for EtOH and $C_{IL}[w/w] = 3.9617 * 10^{-06} * Cond.[\mu S]^{1.041}$ for 2PrOH. With these expressions, the measured conductivity data could be translated into concentrations in the coagulation liquids.

DMSO concentration with NMR

NMR spectra were recorded on a Bruker Avance III HD 800 MHz NMR spectrometer (Bruker BioSpin, Rheinstetten, Germany) equipped with a 5 mm TXO cryoprobe. All experiments were recorded at 298 K. NMR spectra were acquired using a Bruker standard water suppression 1D noesygpps1d pulse sequence in which a phase-modulated square-shaped pulse was used for multiple-band selective solvent suppression. The relaxation delay and acquisition time were set to 5 s and 2 s, respectively, which resulted in a total recycle time of 7 s. After the application of 4 DS, 80 FIDs were collected into a time domain with 65,536 (65 k) complex data points using a 20.5187 ppm SW and a receiver gain of 32. The data was acquired automatically using an ICON-NMR (Bruker BioSpin,

Rheinstetten, Germany) and requiring about 10 min per sample. All NMR spectra were phased, baseline-corrected, and integrated using Topspin 3.2 (Bruker BioSpin, Rheinstetten, Germany). For the longest times, the signal of the measurements displayed a plateau (i.e. they were within the method precision of the equilibrium), at which only negligible amounts of DMSO remain in the coagulated material. Therefore, the long-time signal values could be applied as the reference, to translate NMR signals into DMSO concentrations for the shorter times. Because the calculation of diffusion is based only on the ratio between concentrations for the earlier and the longest times, no improvement in precision is gained by using an intermediate reference curve.

Calculations of apparent D s and rate coefficients k

The D_{NS} , $D_{[C2mim][OAc]}$, and D_{DMSO} discussed in this article are the “apparent” values for short times, unless stated otherwise. “Apparent” in this context means that they were evaluated as if they were assumed to remain constant throughout the measurement and were independent of concentration. Under such assumptions, transient diffusion into a coagulating membrane can be described by Fick’s law (Eq. 1) with the initial and boundary conditions (Eqs. 2, 3) for diffusion into an infinite slab. This problem has an analytical solution, the so-called Boltzmann’s solution, Eq. 4.

$$\frac{\partial C}{\partial t} = D \frac{\partial^2 C}{\partial x^2} \quad (1)$$

$$C(0, x) = 0, \quad x \in [0, \infty] \quad (2)$$

$$C(t, x) = 1, \quad x < 0 \quad (3)$$

$$C(x, t) = \operatorname{erfc}\left(x/(tD * 4)^{1/2}\right) \quad (4)$$

Equation 4 is also applicable to membranes of a finite depth, d , for “short” times, i.e. as long as the concentration at the unexposed limit, d , remains unchanged. By integrating Eq. 4 with regard to x over the interval $[0, d]$, an expression for the total influx as a function of time, $M(t)$, is obtained.

Equation 5 is obtained after normalizing, $M(t)$, with its final value, M_{tot} (i.e. $M(\infty)$), and some reorganizing of the terms. The coefficient of diffusivity, D , can be calculated from data on mass transport to or from membranes of limited depth with Eq. 5, but only data for “short” times can be used (see SI of (Hedlund et al. 2017)).

$$D = \left(\frac{M(t)}{M_{tot}} \frac{d}{2} \right)^2 \frac{\pi}{t} = \frac{\pi}{4} (k * d)^2 \quad (5)$$

In Eq. 5, $M(t)$ is the mass of a certain substance that has diffused either in or out of the membrane, which is of thickness d and exposed only from one side, after time t . It is also common to evaluate diffusion rate coefficients, k , using Eq. 6.

In processes in which D varies, such as coagulation, the actual spatial concentration function does not have the shape of the complementary error function. If Eq. 5 is applied to cases in which D varies, the “apparent” D obtained will not be D in its strict sense, but a quantity akin to a mean value of D . However, in one-dimensional transient diffusive processes and if D depends only on concentration, the concentration function $f(z)$ can always be reduced to a function of only the dimensionless variable: $z = (x^2 / (tD * 4))^{1/2}$ (Crank 1979). This allows the evaluation of the same kind of coefficients of propagation, k , and apparent D s, with the same type of mathematical expressions, such as in Eqs. 5 and 6, for all such processes. This is true even for processes in which the actual shape of the spatial concentration function remains unknown, as is generally the case.

$$\frac{M_i(t)}{M_{i_tot}} = k * t^{1/2} \quad (6)$$

The linear relations between $\frac{M_i(t)}{M_{i_tot}}$ and $t^{1/2}$ enable evaluations of their rate coefficients, k . However, the results presented below in Table 2 and Fig. 2 (except for $k_{coagulation}$) were not evaluated using a simple linear fit but by calculating the mean of the slopes based on each data point, individually, within the appropriate range. This was done to achieve a better statistical

understanding and to avoid giving excessive weight to measurements of longer times. Coefficients k can also be found for coagulation rate and NMG by applying Eqs. 7 and 8, respectively, to data.

$$x_c = k_{coagulation} * t^{1/2} \quad (7)$$

$$\text{NMG} = k_{\text{NMG}} * t^{1/2} \quad (8)$$

Net Mass Gain (NMG) is expressed by Eq. 9, where M_0 refers to the entire mass of the solution.

$$\text{NMG} = \frac{\Delta M(t)}{M_0} = \frac{M(t)}{M(0)} - 1 \quad (9)$$

The limited precision in calculating D is mainly due to the uncertainty of d , which we estimated to be no more than ± 0.02 mm. This translates to a possible error of $\pm 12\%$ (cf. larger grey error bars in Fig. 2). It cannot be excluded that the very different viscosities or different cellulose concentrations of the tested solutions can cause some variation in membrane thickness and, thus, some error in the D s calculated.

The data on $M(t)_{\text{DMSO}}$ and $M(t)_{[\text{C2mim}][\text{OAc}]}$ was calculated from the mass of the coagulation liquid and its weight concentrations of DMSO and $[\text{C2mim}][\text{OAc}]$ measured with NMR and conductivity, respectively. A final plateau, observed for the longest times, was used to quantify the normalizing values ($M_{\text{DMSO_tot}}$ and $M_{[\text{C2mim}][\text{OAc}]_tot}$). Equation 10 was used for $M(t)_{\text{NS}}$.

$$M(t)_{\text{NS}} = M_0 * \left(X_{[\text{C2mim}][\text{OAc}]_0} * \frac{M(t)_{[\text{C2mim}][\text{OAc}]}}{M_{[\text{C2mim}][\text{OAc}]_tot}} + X_{\text{DMSO}_0} * \frac{M(t)_{\text{DMSO}}}{M_{\text{DMSO_tot}}} + \frac{\Delta M(t)}{M_0} \right) \quad (10)$$

In Eq. 10, X_{i_0} is the mass fraction of component i in the non-coagulated starting solution, and $\frac{\Delta M(t)}{M_0}$ is the relative change in mass of said solution (Net Mass Gain) during coagulation time, t . Equation 10 derives from the conservation of mass and states that the inflow of non-solvent amounts to the sum of efflux of other components and the change in total mass. The calculation of $M_{\text{NS_tot}}$ is the most complicated parameter to calculate, because $M_{\text{NS_tot}}$ is the mass that could theoretically be contained in the pore volume of the cellulose material that non-solvent diffuses into and it is not always equal to the final pore

Table 2 A summary of the rate and diffusion coefficients evaluated in the present study

Solution designation (wt_EmimAc:wt_DMSO- wt%MCC)	Coagulant	K_IL (g/g√s)	k_NS (g/g√s)	k_DMSO (g/g√s)	k_coag coagulation rate (mm/√s)	NMG (g/g√s)	D _{DMSO} (10 ⁻¹⁰ m ² /s)	D _{EmimAc} (10 ⁻¹⁰ m ² /s)	D _{NS} (10 ⁻¹⁰ m ² /s)
99:1-5%MCC	H ₂ O	0.0476	0.0622	0.0520	0.0433	0.0171	2.60	2.18	3.71
99:1-14.3%MCC	H ₂ O	0.0517	0.0671	0.0563	0.0415	0.0146	3.05	2.57	4.33
99:1-25%MCC	H ₂ O	0.0467	0.0628	0.0526	0.0436	0.0147	2.66	2.10	3.79
50:50-14.3%MCC	H ₂ O	0.0546	0.0649	0.0561	0.0541	0.0060	3.03	2.86	4.05
50:50-14.3%MCC	2PrOH	0.0235	0.0405	0.0404	0.0271	0.0015	1.57	0.529	1.58
99:1-14.3%MCC	EtOH	0.0280	0.0417	0.0384	0.02823	0.0174	1.42	0.755	1.67
99:1-5%MCC	2PrOH	0.0194	0.0323	0.0341	0.0213	0.0190	1.12	0.361	1.01
99:1-14.3%MCC	2PrOH	0.0182	0.0348	0.0292	0.02022	0.0197	0.82	0.319	1.16
99:1-25%MCC	2PrOH	0.0158	0.0271	0.0447	0.0145	0.0097	1.92	0.241	0.706

Those of water from the previous study (Hedlund et al. 2017) are included for comparison

volume after very long times, due to deswelling when the solvent leaves. Obviously, such later volume changes should not affect diffusion at very short times, i.e. the time range for which the non-solvent diffusion coefficient, D_{NS} , is to be calculated. Thus, M_{NS_tot} became a particularly complex issue for coagulated solutions that exhibited a pronounced loss of mass for the longest times. For this reason, Eq. 11 for the corrected final value of the mass transport of non-solvent, although similar to Eq. 10, uses the maximum NMG value $\left(\frac{\Delta M(t)}{M_0}\right)_{t_{max}}$ instead of the final value $\left(\frac{\Delta M(t)}{M_0}\right)_{t_{final}}$ and ρ_{NS}/ρ_{max} to compensate for the difference in density between non-solvent–solvent mixture at t_{max} and pure non-solvent at t_{final} . Thus, Eq. 11 describes the mass of non-solvent containable in the available volume prior to the structural changes that can take place during washout. Without structural and volume changes, these modifications in Eq. 10 to generate Eq. 11 cancel each other out.

$$M_{NS_tot} = \left[M_0 * (X_{[C2mim][OAc]_0} + X_{DMSO_0} + \frac{\Delta M(t)}{M_0}\right)_{t_{max}} \right] * \frac{\rho_{NS}}{\rho_{max}} \quad (11)$$

Here, the expression inside brackets represents the mass of the liquid phase at the time of maximum NMG (t_{max}). This maximum approximately coincides with the time at which coagulation has penetrated the full depth of the membrane, i.e. when the separation into

liquid and solid phases is complete. By multiplying the mass of the liquid phase by ρ_{NS}/ρ_{max} , we obtain the mass of pure non-solvent that could theoretically be contained in the same volume. However, ρ_{NS}/ρ_{max} is not easily obtainable because the exact composition at t_{max} is unknown. The loss in mass during the subsequent stage of solvent washout appears to be because the densities of the pure non-solvents are lower than their mixtures with [C2mim][OAc]. ρ_{NS}/ρ_{max} was, therefore, approximated based on the mean decrease in NMG from t_{max} to t_{∞} for all the alcohols. If based on data available only for EtOH, ρ_{NS}/ρ_{max} could have been slightly lower, depending on the concentration assumed at t_{max} (Quijada-Maldonado et al. 2012).

Results and discussion

When solutions coagulate, their non-solvent contents increase and their contents of [C2mim][OAc] and DMSO decrease. Figure 1 shows an example of the time dependences of these concentrations, averaged over the entire membrane, as well as the total mass of the coagulating sample. Table 2 is a summary of the mass-transport- and coagulation rate coefficients, k_i , and apparent diffusion coefficients, D_i , obtained for the systems studied in this work, together with previously reported data for coagulation in water.

With 2PrOH and EtOH as coagulants, there are some deviations from the generally expected behavior

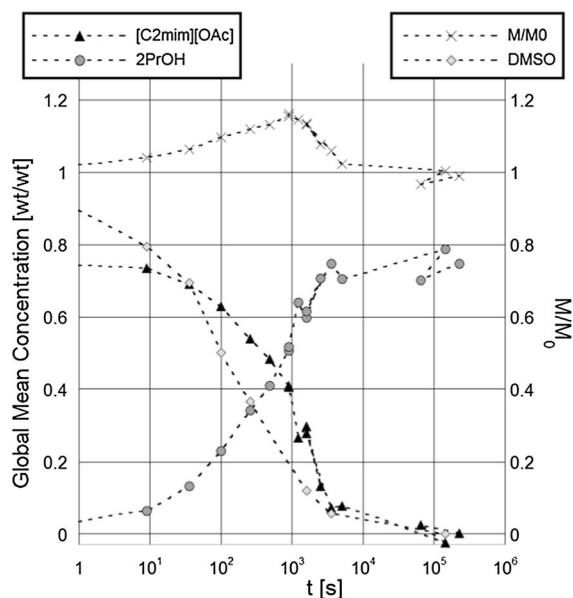


Fig. 1 An example of the 50:50-14.3%MCC solution coagulated in 2PrOH. Note how the weights of each compound and the total mass of the solution relative to its initial mass change with time. The dotted lines serve only to indicate the theoretical starting points of each series

described by Eq. 6. In particular, the diffusion of [C2mim][OAc] appeared to be slower for the shortest times, which means that if $k_{[C2mim][OAc]}$ is evaluated based on those times, it will be lower. A similar observation was made with water as the coagulant, but this observation is more evident and general for the alcohols. Since [C2mim][OAc] interacts strongly with cellulose, a plausible explanation is that an initial infusion of non-solvent is required to release and mobilize the IL before the IL can diffuse out. Similar behavior has been observed for N-methylmorpholine-N-oxide monohydrate cellulose solutions coagulated in water (Laity et al. 2002). In contrast, the diffusion of DMSO appeared to be faster for the shortest times, in 2PrOH. These deviations from linearity to $t^{1/2}$ were handled by using only the middle range of times, at which the ratio of $\frac{M_i(t)}{M_{tot}}/t^{1/2} = k_i$ was stable, which generally corresponds to times for which $0.15 > \frac{M_i(t)}{M_{tot}} > 0.7$. In most cases, this yielded reliable values of k with small standard deviations. However, the resulting values for D_{DMSO} in the solutions with only tracer amounts of DMSO (99:1-[5-25] %MCC) were not as conclusive. This was particularly true for the highest cellulose concentration (99:1-25%MCC)

because in the above cases there was no satisfactory plateau but rather a gradual decrease in D_{DMSO} . The D_{DMSO} of the 50:50-14.3%MCC solution was independent of the times chosen and, therefore, was more reliable.

Diffusion coefficients

Figure 2 shows the diffusion coefficients obtained for coagulation in the two alcohols and a comparison to the corresponding coefficients for coagulation in water. There are several differences. First, the D_{NS} , $D_{[C2mim][OAc]}$, and D_{DMSO} during coagulation in alcohols were lower in all cases. The diffusion during EtOH coagulation was significantly faster than in 2PrOH, but still far below diffusion in water. Second, D_{NS} , $D_{[C2mim][OAc]}$, and D_{DMSO} increased significantly with DMSO content in the solvent during coagulation in alcohol, whereas the effects of DMSO on diffusion during coagulation in water were moderate. Although the data on D_{DMSO} was of limited precision, it clearly showed that D_{DMSO} is the diffusion coefficient that is least dependent on the choice of non-solvent. DMSO, in contrast to [C2mim][OAc], maintained a relatively high diffusive rate also in 2PrOH. Third, with 2PrOH, both D_{NS} and $D_{[C2mim][OAc]}$ were $> 30\%$ lower for the highest cellulose concentration (25 wt%) than for the lowest (5 wt%). The cellulose-concentration independence of the apparent diffusion coefficients during coagulation in water was one among several observations that lead to the main conclusion of our previous article (Hedlund et al. 2017): diffusive mass transport, during coagulation in water, mainly occurs in the liquid phase that has separated from the cellulose solid phase during coagulation. In solutions not yet coagulated, $D_{[C2mim][OAc]}_{self}$ should be about 20 times lower with 25 wt% than with 5 wt% cellulose (Lovell et al. 2010; Ries et al. 2014). Consequently, the observed reduction of only 30% in $D_{[C2mim][OAc]}$ does not contradict, but shows that the conclusion of our previous article (Hedlund et al. 2017) also largely applies to alcohols. The observation that the diffusion coefficients D_i s were in the same order of magnitude as the respective self-diffusion coefficient in dilute non-solvent solutions of [C2mim][OAc], also for the present results with alcohols, constitutes further support.

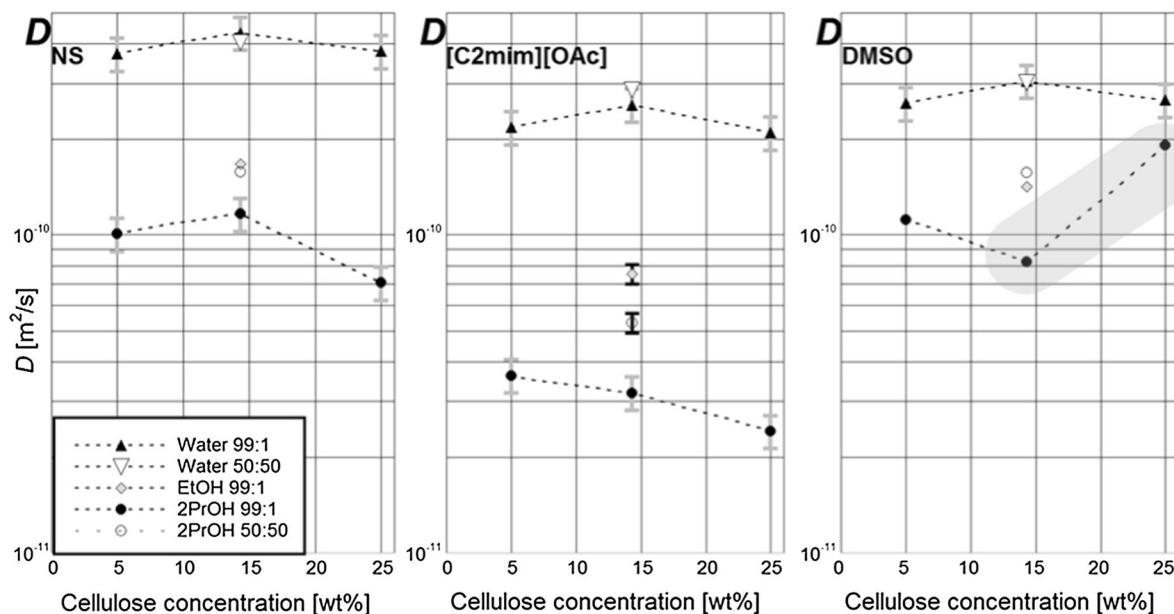


Fig. 2 Apparent diffusion coefficients (D_{NS} , $D_{[C2mim][OAc]}$, and D_{DMSO}) during coagulation in EtOH and 2PrOH shown in comparison to the previous values for coagulation in water: for the non-solvent, for [C2mim][OAc], and for DMSO. The

numbers 50:50 and 99:1 in the legend refers to the solvent composition of [C2mim][OAc], and DMSO: wt%_{[C2mim][OAc]}: wt%_{DMSO}

Even if the main mass transport mechanism of [C2mim][OAc] is diffusion in the non-solvent there are some differences between alcohols and water regarding interaction with [C2mim][OAc] and particularly with cellulose. The degree of swelling of cellulose in a non-solvent is probably the measure available that corresponds the closest to a mixing enthalpy of cellulose and the non-solvent. Water is a very good cellulose swelling medium, whereas alcohols are very poor (El Seoud et al. 2008). Both water and the two alcohols interact strongly and mix exothermally with [C2mim][OAc], but to significantly varying degrees. The exothermal mixing decrease in the order: water > EtOH > 2PrOH, as can be concluded from the relative vapor pressures and activity coefficients of non-solvent-[C2mim][OAc] mixtures (Verma and Banerjee 2010; Zhao et al. 2006). In this series of decreasing mixing enthalpy, cellulose would be expected to place itself close to the alcohols: water > cellulose > EtOH > 2PrOH, based on the the Hansen solubility parameters (HSP), octanol–water partition coefficients (K_{OW}) and hydrogen bond donor ($\alpha\alpha$) or acceptor ($\beta\beta$) parameters in Table 3. The polar HSP and K_{OW} even suggest that cellulose would rank above water. However the combining of

hydrogen bond acceptors and donors is exothermal and dominate other weaker interactions (Liu et al. 2010). Therefore, water ranks on top due to its very high $\alpha\alpha$, which cellulose does not have.¹ A comparison of the mixing enthalpy of water in [C2mim][OAc], 35 kJ/mol water, (Shi et al. 2012) to that of cellobiose in [C4mim][OAc], 19 kJ/mol anhydroglucose units, (de Oliveira and Rinaldi 2015) confirms this. The order of affinity for [C2mim][OAc] is decisive for the way [C2mim][OAc] is divided between the cellulose and non-solvent phases formed during the initial phase separation. This measure translates into a sorption of [C2mim][OAc] by the cellulose phase, a sorption that is much greater in alcohols than in water. The sorption of [C2mim][OAc] implies two things: first, a larger volume fraction is occupied by the cellulose phase, which is effectively both obstructive to and inactive in mass-transport (henceforth the “obstructive-inactive volume” effect, exemplified in Fig. 3), and second, the immobilization of the sorbed [C2mim][OAc]. The first effect is

¹ The hydroxyl groups of cellulose cannot be very much stronger hydrogen-bond donors than other alcohols are (e.g. methanol has $\alpha\alpha = 0.43$ and ethandiol has $\alpha\alpha = 0.58$).

Table 3 Selected parameters that relate to relative affinities of compounds

	Hansen solubility parameters (Hansen 2007)			Octanol–water partition coefficient (CRCnetBASE 1978)	Hydrogen bond donating/accepting solvatochromic parameters (Abraham et al. 1994)	
	Dispersion	Polar	Hydrogen bond		$\alpha\alpha$ (donor)	$\beta\beta$ (acceptor)
Cellulose	24.3 (Dextran)	19.9 (Dextran)	22.5 (Dextran)	– 2.8 (glucose) (Mazzobre et al. 2005)		
Water	15.5	16.0	42.3	– 1.38 (Oliferenko et al. 2004)	0.82	0.35
EtOH	15.8	8.8	19.4	– 0.3	0.37	0.48
2PrOH	15.8	6.1	16.4	0.05	0.33	0.56
DMSO	18.4	16.4	10.2	– 1.35	0	0.88
[C2mim][OAc]				– (2 to 2.5) (Montalbán et al. 2015)	($\alpha = 0.5$ Kamlet-Taft) (Hauru et al. 2012)	($\beta = 1.1$ Kamlet-Taft) (Hauru et al. 2012)

Dextran and glucose have relevant similarities to cellulose with regard to these aspects and supply approximations in lack of data on actual cellulose. The polar Hansen solubility parameter and K_{OW} both indicate that water and cellulose have significantly greater affinity for [C2mim][OAc] than the alcohols have

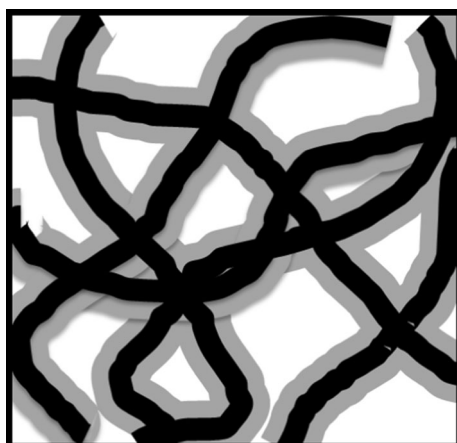


Fig. 3 A schematic visualization of the larger obstructive effect on mass transport from the solid phase, which can result if the cellulose fibrils are swollen (grey) by absorbed [C2mim][OAc], compared to the effect from compact fibrils (black), without [C2mim][OAc]

general and should affect all diffusing components equally, whereas the second is selective towards [C2mim][OAc]. Additional indirect consequences of [C2mim][OAc] sorption could also generate counter-acting effects, which would reduce the total effect observed. In particular, the diffusivities in the non-solvent phase are negatively affected by a high [C2mim][OAc] concentration. Thus, the reduced

diffusion, due to a reduction in non-solvent phase volume, can to some extent be compensated by a locally increased diffusivity in the non-solvent phase when [C2mim][OAc] is confined to the obstructive cellulose phase.

Non-solvent diffusion

Diffusion during coagulation is limited to a continuous phase composed of non-solvent and solvent. Because the non-solvent self-diffusion coefficient, D_{NS_self} , should describe diffusion in the outer parts of that non-solvent phase with low [C2mim][OAc] concentrations, it is pertinent to compare D_{NS} to D_{NS_self} to analyze the effects of [C2mim][OAc] and cellulose on diffusion. Figure 4 shows the ratios of D_{NS}/D_{NS_self} , which are relatively well-contained around $0.175 \pm 10\%$, except for the 50:50-14.3%MCC and 99:1-25%MCC solutions coagulated in 2PrOH. This constant ratio indicates that the non-solvent molecule's mobility is the primary underlying parameter that affects the apparent D_{NS} during coagulation. There are two effects that can explain the reduced D_{NS}/D_{NS_self} ratio in the most concentrated solution (99:1-25%MCC). First, the general “obstructive-inactive volume” effect from cellulose sorption of [C2mim][OAc] increases as the amount of cellulose

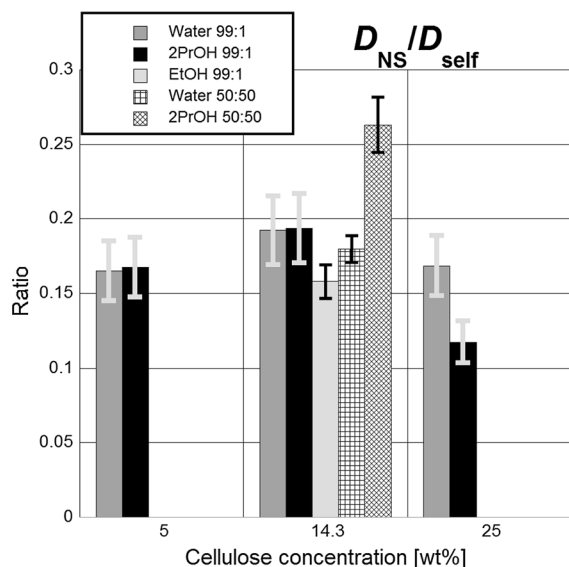


Fig. 4 The apparent diffusion coefficients of the non-solvent D_{NS} divided by the non-solvents' respective self-diffusion coefficients: 2.23, water; 1.06, EtOH; and $0.6 \times 10^{-9} \text{ m}^2/\text{s}$, 2PrOH, according to NMR data (Gillen et al. 1972; Hurle et al. 1985; Meckl and Zeidler 1988; Partington et al. 1952)

increases relative to the amount of infusing non-solvent. If it is assumed that [C2mim][OAc] is divided locally between the non-solvent and cellulose phases in proportion to their respective weights, the non-solvent-phase volume fraction of a newly coagulated volume element is very small in solutions with the highest cellulose concentrations, which also require very little non-solvent to coagulate (low CVs). After phase separation, the volume fraction of non-solvent phase will gradually increase, as more non-solvent diffuses in, but this process is very slow if the volume, through which the diffusion is conducted, is very small. Therefore, the cellulose phase can be expected to be the dominant volume fraction in the 25 wt% cellulose solution until non-solvent concentrations are many times the CV (8 wt%), as with 2PrOH. The difference in D_{NS}/D_{NS_self} between water and 2PrOH is due to a difference in the proportions by which [C2mim][OAc] is divided between cellulose and non-solvent. In water, very little [C2mim][OAc] remains in the cellulose phase (Hedlund et al. 2017). Second, there is approximately one cellulose OH group per acetate ion in 25 wt% cellulose solutions. Because the [C2mim][OAc] anions hydrogen-bond to these OH groups, the IL solvent anions have very low mobility, beyond the coagulation front in 25 wt% cellulose

solutions. Anions hydrogen-bonded to cellulose are about 50 times less mobile than anions in pure solvent (Ries et al. 2014). Henceforth, this concept will be referred to as “solvent saturation.” In most solutions of polymers in simple molecular solvents, such as water, acetone, benzene, tetrahydrofuran, and others, there is a transition polymer concentration around 0.4 g/g at which solvent diffusion decreases dramatically faster with increased polymer concentration (Phillies 2011). That author explains the transition by the retarding effect on solvent mobility induced by a polymer chain within 1 to 2 solvent molecule radii from itself. At the transition concentration, there is essentially no unaffected solvent volume left, which dramatically reduces mobility. That this would happen at a concentration lower than 0.4 g/g in [C2mim][OAc]-cellulose solutions is not surprising given the large M_w of the solvent [C2mim][OAc] and in particular the much stronger interactions. The hydrogen bonds and ionic interactions in ILs are much stronger than the Van der Waals dominated interactions between most synthetic polymers and their molecular solvents. Further, the effect of this transition on small-molecule diffusion increases with the size of the diffusing molecule. Consequently, the difference in molecular size is probably at least part of the reason why the same trend in D_{NS} was not found for coagulation in water. As described in Diffusion Coefficients, compatibility with the cellulose-[C2mim][OAc] solution, which is a non-solvent property akin to solubility, is better for water than for 2PrOH. Based on the dramatic reduction in diffusivity generally incurred by “solvent saturation,” its effect on apparent diffusion can be expected to be much larger than the decrease in D_{NS} actually observed. The reason that a dramatic effect was not observed, is probably that the concept of “solvent saturation” is valid only at and beyond the coagulation front, where there is a single solution phase. Consequently, “solvent saturation” does not directly affect diffusion through the liquid volume of the already phase-separated zone, which contains most of the concentration difference. “Solvent saturation,” i.e. the inhibiting effect on diffusion through the coagulation front, affects the rate of non-solvent mass transport through the coagulated zone by redistributing part of the concentration difference from the coagulated zone to the coagulation front. This is demonstrated in Fig. 5, which shows two example curves for the

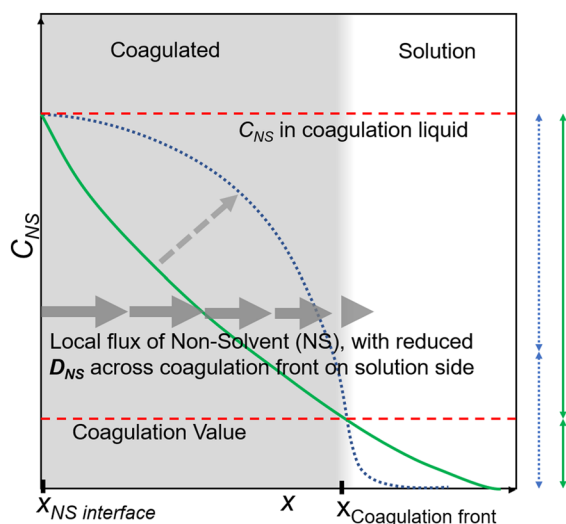


Fig. 5 Examples of how concave (green) and convex (blue) non-solvent concentration curves can cause coagulation at the same depth, but with different total amounts of non-solvent diffused into the coagulating solution. Grey arrows, which represent diffusive fluxes, illustrate the effect of reduced diffusivity at the coagulation front and the accumulation of non-solvent behind the coagulation front. The arrows to the right indicate different divisions of the non-solvent concentration difference between the coagulated ($\Delta C_{NS,coag}$) and not coagulated ($\Delta C_{NS,front}$) zones for the two example curves. (Color figure online)

distribution of non-solvent and how the total non-solvent concentration difference, ΔC_{NS} , can be divided differently in the coagulated zone, $\Delta C_{NS,coag}$, and the front, $\Delta C_{NS,front}$ (not coagulated part), depending on the existence of local drop in diffusivity. As a consequence, the concentration gradient is reduced in the coagulated zone and the non-solvent concentration builds up close to the coagulation front. Because diffusivity increases greatly with non-solvent content, the effect from the smaller concentration gradient is compensated by the higher diffusivity incurred by the built up non-solvent concentrations. Due to such feedback effects and other complexities, it is difficult to estimate the aggregated importance of the “solvent saturation” effect or to quantify its importance relative to the “obstructive-inactive volume” effect. “Solvent saturation” combined with the “obstructive-inactive volume” effect produce the observed drop in non-solvent mobility for the 99:1–25%MCC solution if coagulated in 2PrOH.

The D_{NS} of the 50:50–14.3%MCC solution coagulated in 2PrOH is larger than the D_{NS} of the 99:1–

14.3%MCC, and several factors can explain this. First, the mobility of molecules increases with DMSO content, both in the phase-separated and in the still-dissolved zone (Radhi et al. 2015). However, DMSO can be expected to have a more drastic effect on mobility in the still-dissolved zone, where the DMSO is much more mobile than the other major compounds, i.e. [C2mim][OAc] and cellulose. 2PrOH does not interact as strongly with DMSO as water does, and it has a self-diffusivity similar to that of DMSO (Partington et al. 1952; Radhi et al. 2015). Second, the addition of DMSO reduces the CVs for 2PrOH considerably, from 0.25 g/g for 99:1–14.3%MCC to 0.17 g/g. This can accelerate diffusion by increasing the rate at which the coagulation front advances. This happens because less non-solvent must diffuse into induce coagulation and diffusion is faster in the coagulated zone. The reduction in CV is smaller for water, from 0.14 to 0.11. A possible third effect relates to the way DMSO is divided between the 2PrOH- and cellulose-rich phases, relative to how [C2mim][OAc] is divided between these phases. If DMSO prefers the non-solvent phase, both the volume fraction of non-solvent phase and its diffusion coefficient will increase. Very little is known about how DMSO would divide between the phases, and, thus, not even the sign (\pm) of this third effect can be anticipated.

In summary, it can be expected that the initial presence of DMSO counteracts the resistance to diffusion that the coagulation front generates. DMSO does so by reducing the difference in mobility between the solution and its coagulated material, i.e. by increasing the mobility more in the solution, and by forcing the barrier that the coagulation front constitutes to retreat at a faster pace, due to lower CVs.

[C2mim][OAc] diffusion

The apparent diffusion coefficients of [C2mim][OAc] can be expected to be proportional to the apparent diffusion coefficients of the non-solvents due to close links between these parameters; the release of [C2mim][OAc] from cellulose is dependent on non-solvent infusion and coagulation, i.e. phase separation, which typically precedes the outward diffusion of [C2mim][OAc]. An approximation of the diffusion of [C2mim][OAc] based on the Stokes–Einstein equation for spherical particles diffusing in dilute solutions would predict only moderate differences in

$D_{[C2mim][OAc]}$ of little more than 2 times, between the coagulation in the alcohols and in water, given their viscosities: water, 0.89; EtOH, 1.074; and 2PrOH, 2.038 mPas. However, the $D_{[C2mim][OAc]}$ s during 2PrOH coagulation are 6 to 9 times lower than the values previously reported for water. With more DMSO in the solvent, or with EtOH as the non-solvent, the ratio ($D_{[C2mim][OAc]in\ water}/D_{[C2mim][OAc]in\ alcohol}$) is smaller at 5.4 and 3.3 times, respectively. In all cases, the differences are significantly larger than could be expected, based on the D_{NS} s or available viscosity- or self-diffusivity data. The larger differences between $D_{[C2mim][OAc]}$ and D_{NS} are emphasized by their ratios in Fig. 6. The $D_{NS}/D_{[C2mim][OAc]}$ ratio depends mainly on the non-solvent compound. Based on the relative molecular weights of non-solvent and the ions of $[C2mim][OAc]$, the more similarly sized species, 2PrOH and $[C2mim][OAc]$, would be expected to have the smallest ratio. However, Fig. 6 clearly shows the opposite; water has the lowest ratio: $D_{NS}/D_{[C2mim][OAc]} \approx 1.7 < \approx 2.2$, EtOH, $< \approx 3$, 2PrOH. The explanation for these different ratios has two parts, but both are consequences of the relative affinity of $[C2mim][OAc]$ for the other compounds, as discussed above. Its affinity decreases in the order: water > cellulose > EtOH > 2PrOH, as concluded

from Table 3 and the discussion in Diffusion Coefficients. Thus, water easily detracts $[C2mim][OAc]$ from the cellulose whereas the alcohols, and 2PrOH in particular, attract $[C2mim][OAc]$ but to a lesser degree, leaving a large part of the $[C2mim][OAc]$ sorbed by the cellulose. The part sorbed by cellulose does not diffuse through the non-solvent phase during coagulation in alcohols. The first part of the explanation is the delayed diffusion of $[C2mim][OAc]$ from the not yet coagulated solution. The second part is the sorption of $[C2mim][OAc]$ by the cellulose in the coagulated and phase-separated material. This effect is very selective for $[C2mim][OAc]$ and effectively reduces both the concentration and the gradient of $[C2mim][OAc]$ in the diffusing non-solvent phase.

This explanation, which relates to cellulose content, could be considered with skepticism given the lower $D_{NS}/D_{[C2mim][OAc]}$ ratio for the highest cellulose concentration (99:1-25%MCC) compared to the lower concentration (99:1-14.3%MCC) in 2PrOH. However, the low D_{NS} and low coagulation rate (see Coagulation Rate Coefficients) for the highest cellulose concentration (99:1-25%MCC) mean that the coagulated volume is more thoroughly washed out before new material is coagulated. For example, if the coagulation front inhibits the diffusion of the non-solvent beyond it, there will be both higher non-solvent concentrations (higher diffusivities) in the non-solvent phase and more time for the washout of $[C2mim][OAc]$ from the cellulose-rich phase that the front leaves behind.

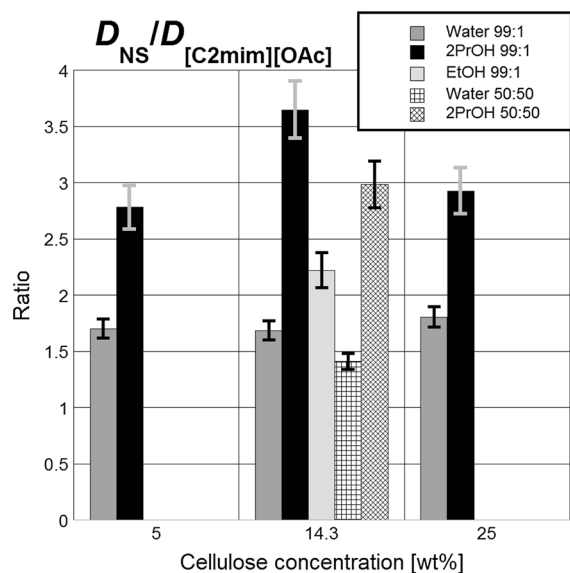


Fig. 6 The ratios of the apparent diffusion coefficients of non-solvent and of $[C2mim][OAc]$

Coagulation rate coefficients

The coagulation rate coefficients k_{coag} in Table 2 generally correlate well with the D_{NS} , which is expected given that non-solvent infusion induces coagulation. In previous work on coagulation rates and diffusion (Biganska and Navard 2005; Hauru et al. 2016), k_{Coag} has been used to calculate D_{NS} based on Eq. 12. In our previous article, we showed that Eq. 12 gives an exaggerated value by a factor in the order of 4 (Hedlund et al. 2017).

$$D_{NS} = \frac{\pi}{4} (k_{coag} * d)^2 \quad (12)$$

However, from a mathematician's perspective, D_{NS} calculated by Eq. 12 and k_{Coag} actually describes the spreading ("diffusion") of coagulated volume if "coagulated volume" is hypothetically imagined to

be a “substance.” This quantity, although somewhat theoretical, is of interest for comparisons with the diffusion coefficients of the real diffusing substances and will be termed D_{coag} . The ratio $(D_i/D_{\text{coag}})^{1/2}$, is a measure of the change in the mean concentration of component i in the coagulated volume (assuming that mass transport is limited to the coagulated zone, which is often a decent approximation). $(D_i)^{1/2}$ quantifies the mass flux of component i and $(D_{\text{coag}})^{1/2}$ quantifies the volume penetrated by said diffusive flux. Therefore, the ratio of these two quantities amounts to a change in concentration. The ratio of infused non-solvent per coagulated volume, $(D_{\text{NS}}/D_{\text{coag}})^{1/2}$, (see Fig. 7) is the most interesting of these ratios because of the role of non-solvents in inducing coagulation. The non-solvent distribution curve declines in the coagulated zone from the exterior concentration to the concentration at the coagulation front, the CV, as shown in Fig. 5. Because the curve must be smooth and decline over the whole range, high ratios indicate more convex curves, blue in Fig. 5, and low ratios concave curves, green in Fig. 5, at constant CVs and cellulose concentrations. The lower CVs of the higher cellulose concentrations imply that both the start and the end concentrations of the curve decrease with increasing cellulose concentration. Therefore, higher CVs should

imply a less convex non-solvent concentration curve for a given $D_{\text{NS}}/D_{\text{coag}}$ ratio. Both CVs and $D_{\text{NS}}/D_{\text{coag}}$ are higher for 2PrOH than for water, but increasing cellulose concentrations coagulated in 2PrOH show a negative correlation between CVs and $D_{\text{NS}}/D_{\text{coag}}$. Thus, it appears that solutions coagulated in 2PrOH have significantly more convex non-solvent concentration curves if their cellulose concentrations are higher. Constant diffusivities give concave concentration distribution functions, i.e. complimentary error functions, for transient processes, whereas convex functions follow from diffusivities that decline with distance from the interface. Any local decline in diffusivity induces a drop in concentration ahead of it and an increase in concentration behind it. Consequently, the most likely parameter to explain the variations in the $D_{\text{NS}}/D_{\text{coag}}$ is the diffusive resistance of the non-coagulated solution, which increases with cellulose concentration. Therefore, the observed increase in $D_{\text{NS}}/D_{\text{coag}}$ with cellulose concentration supports the “solvent saturation” concept proposed to explain the low D_{NS} for 99:1-25%MCC in 2PrOH. This would produce a local decline in non-solvent diffusivity.

The differences in $D_{\text{NS}}/D_{\text{coag}}$ between different non-solvents are smaller for 14.3 wt% cellulose solutions, which is in line with “solvent saturation” being mainly effective at the highest concentrations. For example, that $D_{\text{NS}}/D_{\text{coag}}$ for EtOH is lower than for water is the opposite of what would have been expected from the “solvent saturation” effect. This indicates that “solvent saturation” is not very important at medium and lower cellulose concentrations. However, the lower ratios for the solutions with more DMSO (50:50-14.3%MCC) are a likely consequence of DMSO’s disruption of the “solvent saturation” effect, which may indicate that the effect is still of some importance. DMSO could provide both the additional mobility and vacant space for 2PrOH to enter. This would reduce the drop in non-solvent diffusivity over the coagulation front. Water interacts very well with DMSO and the CVs of water are not much reduced by the use of DMSO as a co-solvent. Thus, water in particular is likely to be present in the solution beyond the coagulation front and further increase the diffusivity there.

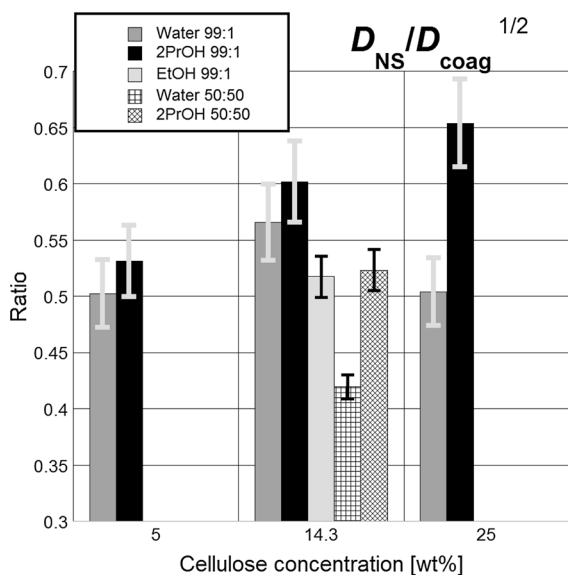


Fig. 7 The ratio of the diffusion coefficient D_{NS} and D_{coag} , which constitutes a measure of the compactness of non-solvent distribution

Net mass gain

Figure 8a, b show the change in mass relative to the initial solution mass over time during coagulation. As previously described for water (Hedlund et al. 2017), all curves represent the same two stages. The NMG increases during coagulation and decreases during washout. The NMG_{\max} at the transition between coagulation and precipitation is a value that probably influences the structural properties of the coagulated material. This is because it translates into a factor of polymer dilution at a time when solid structures start to set (Hedlund et al. 2017). The NMG_{\max} values increase in the order: $2\text{PrOH} > \text{EtOH} > \text{H}_2\text{O}$. They correlate approximately to coagulation values, CVs. The CVs would provide a logical explanation for variations in NMG, because the $[\text{C2mim}][\text{OAc}]$ is not very mobile prior to phase separation, which is incurred when the amount of non-solvent prescribed by the CV has entered an incremental volume of the solution. Thereafter, the opposing diffusive volume fluxes of non-solvent and $[\text{C2mim}][\text{OAc}]$ are more balanced. This makes the CV a central parameter that influences the NMG_{\max} . With 2PrOH as the non-solvent, there is also a clear decreasing trend in NMG_{\max} with increasing cellulose concentration. This too is consistent with the dependence on CV.

However, the variations in NMG_{\max} are much smaller than the corresponding variations in CV. The correlation to CVs is not generally valid when different non-solvents are compared. This is exemplified by the coagulation of 99:1-14.3%MCC in water ($\text{NMG}_{\max} \approx 0.1$ and $\text{CV} = 14 \text{ wt\%}$) compared to 99:1-25%MCC in 2PrOH ($\text{NMG}_{\max} \approx 0.15$ and $\text{CV} = 8 \text{ wt\%}$). The existence of some additional factor that is more dependent on the non-solvent compound than on the cellulose concentration is indicated. This factor reduces the difference between NMG_{\max} values for different cellulose concentrations. It is notable that the 99:1-25%MCC solution coagulated in 2PrOH has a large NMG_{\max} value, which implies that the local NMG_{\max} , always higher than the global (mean) NMG_{\max} , is several times the CV. The lower limit of the local NMG_{\max} can be obtained from Eq. 13. For details, see our previous article (Hedlund et al. 2017).

$$\left[\frac{\Delta M(t)}{M_0} \right]_{\max} = \left[\frac{\Delta M(t)}{M_0} \right]_{\text{tot}} \frac{x_{\text{coag.}}}{(x_{\text{coag.}} - x_{\text{wash-out}})} - \left[\frac{\Delta M(t)}{M_0} \right]_{\text{final}} \frac{x_{\text{wash-out}}}{(x_{\text{coag.}} - x_{\text{wash-out}})} \quad (13)$$

A possible explanation for the local NMG_{\max} being able to exceed the CV, is that a given amount of a certain non-solvent must be absorbed before the

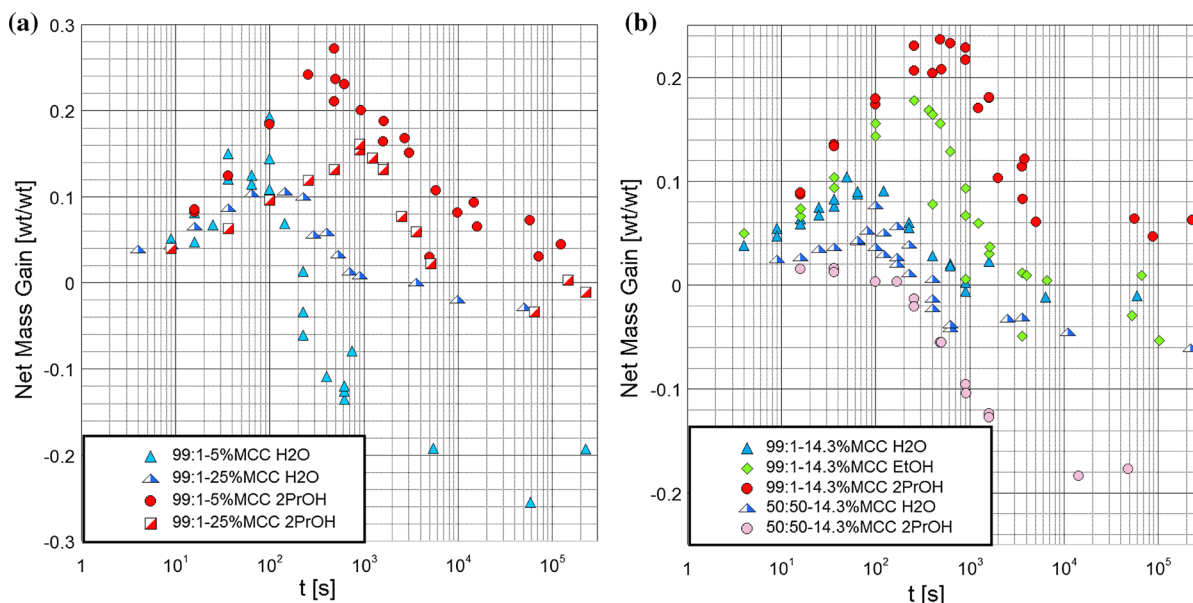


Fig. 8 NMG as a function of time. The two phases of initial non-solvent absorption during coagulation and secondary mass-loss during washout are shown

washout of the [C2mim][OAc] solvent can balance the influx of non-solvent, in particular if the cellulose concentration is high. Laity (Laity et al. 2002) have observed that the non-solvent frees the solvent from the cellulose and mobilizes it. During washout, the volume appears to be largely maintained as the decrease in mass matches the difference in density between the non-solvent-[C2mim][OAc] and the pure non-solvent. Thus, the amplitude of the decrease in mass during washout is larger for the alcohols than for water. The exception is the 99:1-5% MCC solution, the volume of which shrunk about 20% in water but not significantly in 2PrOH during the washout phase. An addition of DMSO to the solvent composition is the most efficient way to reduce the NMG, as previously found for coagulation in water. It appears that DMSO is even more effective in 2PrOH, probably because of the relatively similar self-diffusivities and molecular volumes of DMSO and 2PrOH. With DMSO leaving and 2PrOH entering at similar rates, coagulation can be induced without any significant NMG. However, there is a local $NMG_{max} > 5\%$, as can be concluded from Eq. 13 and the lower final level of NMG ($\approx -18\%$).

Mass transport effects on microstructures

One objective of this research was to find effects from the mass transport during coagulation on the resulting material properties. In a previous paper (Hedlund et al. 2019), the crystalline order of coagulated and solvent exchanged dry material was found to decrease with increasing cellulose concentration for coagulation in water. In contrast, the crystalline order remained constant and very low, almost amorphous, for all solutions coagulated in 2PrOH. The addition of DMSO to the solvent also reduced the crystalline order for coagulation in water, whereas DMSO had no effect in 2PrOH. The specific surface areas, SSAs, increased with cellulose concentration: slightly in 2PrOH, from 270 to 300 m²/g; and significantly in water, from 300 to 370 m²/g. Correlations of these to mass-transport parameters are not evident. For example, the rather constant mass transport rates in all four solutions coagulated in water do not explain the variations in crystalline order and SSAs. The opposite was observed in 2PrOH; variable mass transport rates and a constant, low, crystalline order of the material formed. Constant parameters are poor explanations for

variable values and vice versa. An example in which both parameters actually vary is the comparison of the non-solvents, water and 2PrOH. However, in that case, it appears that lower coagulation and mass-transport rate would generate lower crystalline order. This positive correlation between crystallinity and coagulation rate is contrary to general knowledge about polymer crystallinity and crystallization rate.

In summary, it seems that microstructures and the ability of cellulose macromolecules to organize themselves in large fibrils or large crystalline domains is mainly due to other issues than mass-transport and coagulation rates, such as the local conditions at which the organizing takes place.

Conclusions

In this study we found that the apparent diffusion coefficients of the non-solvents, D_{NSS} , during the coagulation of [C2mim][OAc]-cellulose solutions are proportional to ($\approx 1/6$ th of) the self-diffusivity of each non-solvent. This indicates that, during coagulation in alcohol, mass transport is limited to a continuous non-solvent phase that is separated from cellulose during coagulation, similar to coagulation in water. However, there are apparent differences from what has been observed for coagulation in water. The mass-transport rates decrease with increased cellulose concentration with 2PrOH as the non-solvent. The net mass gain is significantly larger during coagulation in alcohols. This is because the diffusive flux of non-solvent is greater than the diffusive flux of [C2mim][OAc], which is particularly sensitive to the type of non-solvent compound. During coagulation in alcohols, the diffusion of [C2mim][OAc] was much slower than could be expected based on the self-diffusivities and viscosities of the non-solvents. The ratios of non-solvent diffusive rates and coagulation rates remained relatively constant for the different non-solvents and different solutions. This confirms that non-solvent diffusion controls the rate of coagulation. However, the ratio was higher for coagulation in 2PrOH, which revealed that the infusion of 2PrOH as non-solvent is more concentrated to the coagulated parts than is water as non-solvent. These differences arose because [C2mim][OAc] remains partly sorbed by and immobilized in the cellulose phase, if the non-solvent affinity for [C2mim][OAc] is not significantly

larger than the affinity of cellulose for [C2mim][OAc]. The interactions between [C2mim][OAc] and cellulose are more persistent in alcohols than in water, which interact more strongly with [C2mim][OAc] than alcohols do. During coagulation in 2PrOH, the mass transport of both non-solvent and [C2mim][OAc] was particularly inhibited by high cellulose concentrations that approached the solubility limit, because of the increasing difficulty for non-solvent molecules to penetrate into the not-yet-coagulated solution. The difficulty of non-solvent molecules to penetrate into the not-yet-coagulated solution increased with their molecular volume and if their affinity for cellulose was poorer. There were no findings to suggest any effects from mass-transport rates on the microstructures formed.

Acknowledgments Open access funding provided by Chalmers University of Technology. This research would not have been possible without financing from the Södra Skogsägarna Foundation for Research, Development and Education. The scientists at the Swedish NMR Centre in Gothenburg as well as the other partners within the Avancell Project are gratefully acknowledged for their help in this Project.

Open Access This article is distributed under the terms of the Creative Commons Attribution 4.0 International License (<http://creativecommons.org/licenses/by/4.0/>), which permits unrestricted use, distribution, and reproduction in any medium, provided you give appropriate credit to the original author(s) and the source, provide a link to the Creative Commons license, and indicate if changes were made.

References

- Abraham MH, Chadha HS, Whiting GS, Mitchell RC (1994) Hydrogen bonding. 32. An analysis of water-octanol and water-alkane partitioning and the $\Delta\log P$ parameter of Seiler. *J Pharm Sci* 83:1085–1100
- Bengtsson J, Olsson C, Hedlund A, Köhnke T, Bialik E (2017) Understanding the inhibiting effect of small-molecule hydrogen bond donors on the solubility of cellulose in tetrabutylammonium acetate/DMSO. *J Phys Chem B* 121:11241–11248
- Biganska O, Navard P (2005) Kinetics of precipitation of cellulose from cellulose-NMMO-water solutions. *Biomacromol* 6:1948–1953
- Crank J (1979) *The mathematics of diffusion*. Oxford University Press, Oxford
- CRCnetBASE (1978) *CRC handbook of chemistry and physics*. CRC Press, Boca Raton
- de Oliveira HFN, Rinaldi R (2015) Understanding cellulose dissolution: energetics of interactions of ionic liquids and cellobiose revealed by solution microcalorimetry. *Chem-suschem* 8:1577–1584
- El Seoud OA, Fidale LC, Ruiz N, D' Almeida MLO, Frollini E (2008) Cellulose swelling by protic solvents: which properties of the biopolymer and the solvent matter? *Cellulose* 15:371–392
- Fink H-P, Weigel P, Purz H, Ganster J (2001) Structure formation of regenerated cellulose materials from NMMO-solutions. *Prog Polym Sci* 26:1473–1524
- Gavillon R, Budtova T (2007) Kinetics of cellulose regeneration from cellulose-NaOH-water gels and comparison with cellulose-N-methylmorpholine-N-oxide-water solutions. *Biomacromol* 8:424–432
- Gillen KT, Douglass DC, Hoch MJR (1972) Self-diffusion in liquid water to $-31\text{ }^{\circ}\text{C}$. *J Chem Phys* 57:5117–5119
- Gupta KM, Hu Z, Jiang J (2013) Cellulose regeneration from a cellulose/ionic liquid mixture: the role of anti-solvents. *RSC Adv* 3:12794–12801
- Hansen CM (2007) *Hansen solubility parameters: a user's handbook*. CRC Press, Boca Raton
- Hauru LK, Hummel M, King AW, Kilpeläinen I, Sixta H (2012) Role of solvent parameters in the regeneration of cellulose from ionic liquid solutions. *Biomacromol* 13:2896–2905
- Hauru LK, Hummel M, Nieminen K, Michud A, Sixta H (2016) Cellulose regeneration and spinnability from ionic liquids. *Soft Matter* 12:1487–1495
- Hedlund A, Köhnke T, Theliander H (2015) Coagulation of EmimAc-cellulose solutions: dissolution-precipitation disparity and effects of non-solvents and cosolvent. *Nord Pulp Paper Res J* 30:32–42
- Hedlund A, Köhnke T, Theliander H (2017) Diffusion in ionic liquid-cellulose solutions during coagulation in water: mass transport and coagulation rate measurements. *Macromolecules* 50:8707–8719. <https://doi.org/10.1021/acs.macromol.7b01594>
- Hedlund A, Köhnke T, Hagman J, Olsson U, Theliander H (2019) Microstructures of cellulose coagulated in water and alcohols from 1-ethyl-3-methylimidazolium acetate: contrasting coagulation mechanisms. *Cellulose* 26:1545–1563
- Hurle RL, Eastale AJ, Woolf LA (1985) Self-diffusion in monohydric alcohols under pressure. Methanol, methanol (2 H) and ethanol. *J Chem Soc Faraday Trans 1 Phys Chem Condens Phases* 81:769–779
- Laity P, Glover P, Hay J (2002) Composition and phase changes observed by magnetic resonance imaging during non-solvent induced coagulation of cellulose. *Polymer* 43:5827–5837
- Liu H, Sale KL, Holmes BM, Simmons BA, Singh S (2010) Understanding the interactions of cellulose with ionic liquids: a molecular dynamics study. *J Phys Chem B* 114:4293–4301
- Lovell CS, Walker A, Damion RA, Radhi A, Tanner SF, Budtova T, Ries ME (2010) Influence of cellulose on ion diffusivity in 1-ethyl-3-methyl-imidazolium acetate cellulose solutions. *Biomacromol* 11:2927–2935
- Mazzobre MF, Román MV, Mourelle AF, Corti HR (2005) Octanol-water partition coefficient of glucose, sucrose, and trehalose. *Carbohydr Res* 340:1207–1211

- Meckl S, Zeidler M (1988) Self-diffusion measurements of ethanol and propanol. *Mol Phys* 63:85–95
- Montalbán M, Collado-González M, Trigo R, Díaz Baños F, Vílora G (2015) Experimental measurements of octanol-water partition coefficients of ionic liquids. *J Adv Chem Eng* 5:1000133
- Oliferenko AA, Oliferenko PV, Huddleston JG, Rogers RD, Palyulin VA, Zefirov NS, Katritzky AR (2004) Theoretical scales of hydrogen bond acidity and basicity for application in QSAR/QSPR studies and drug design. Partitioning of aliphatic compounds. *J Chem Inf Comput Sci* 44:1042–1055
- Olsson C, Hedlund A, Idström A, Westman G (2014) Effect of methylimidazole on cellulose/ionic liquid solutions and regenerated material therefrom. *J Mater Sci* 49:3423–3433
- Östlund Å, Idström A, Olsson C, Larsson PT, Nordstierna L (2013) Modification of crystallinity and pore size distribution in coagulated cellulose films. *Cellulose* 20:1657–1667
- Partington JR, Hudson RF, Bagnall KW (1952) Self-diffusion of aliphatic alcohols. *Nature* 169:583–584
- Parviainen A et al (2013) Predicting cellulose solvating capabilities of acid-base conjugate ionic liquids. *Chemsuschem* 6:2161–2169. <https://doi.org/10.1002/cssc.201300143>
- Phillies GD (2011) Phenomenology of polymer solution dynamics. Cambridge University Press, Cambridge
- Quijada-Maldonado E, Van der Boogaart S, Lijbers J, Meindersma G, De Haan A (2012) Experimental densities, dynamic viscosities and surface tensions of the ionic liquids series 1-ethyl-3-methylimidazolium acetate and dicyanamide and their binary and ternary mixtures with water and ethanol at $T = (298.15 \text{ to } 343.15 \text{ K})$. *J Chem Thermodyn* 51:51–58
- Radhi A, Le KA, Ries ME, Budtova T (2015) Macroscopic and microscopic study of 1-ethyl-3-methyl-imidazolium acetate-DMSO mixtures. *J Phys Chem B* 119:1633–1640
- Remsing RC, Swatoski RP, Rogers RD, Moyna G (2006) Mechanism of cellulose dissolution in the ionic liquid 1-n-butyl-3-methylimidazolium chloride: a ^{13}C and $^{35/37}\text{Cl}$ NMR relaxation study on model systems. *Chem Commun* 12:1271–1273
- Ries ME, Radhi A, Keating AS, Parker O, Budtova T (2014) Diffusion of 1-ethyl-3-methyl-imidazolium acetate in glucose, cellobiose, and cellulose solutions. *Biomacromol* 15:609–617
- Sescousse R, Gavillon R, Budtova T (2011) Aerocellulose from cellulose-ionic liquid solutions: preparation, properties and comparison with cellulose-NaOH and cellulose-NMMO routes. *Carbohydr Polym* 83:1766–1774
- Shi W, Damodaran K, Nulwala HB, Luebke DR (2012) Theoretical and experimental studies of water interaction in acetate based ionic liquids. *Phys Chem Chem Phys* 14:15897–15908
- Swatoski RP, Spear SK, Holbrey JD, Rogers RD (2002) Dissolution of cellulose with ionic liquids. *J Am Chem Soc* 124:4974–4975
- Verma VK, Banerjee T (2010) Ionic liquids as entrainers for water + ethanol, water + 2-propanol, and water + THF systems: a quantum chemical approach. *J Chem Thermodyn* 42:909–919. <https://doi.org/10.1016/j.jct.2010.03.001>
- Wawro D, Hummel M, Michud A, Sixta H (2014) Strong cellulosic film cast from ionic liquid solutions. *Fibres & Textiles in Eastern Europe*, Lodz
- Zhang J, Zhang H, Wu J, Zhang J, He J, Xiang J (2010) NMR spectroscopic studies of cellobiose solvation in EmimAc aimed to understand the dissolution mechanism of cellulose in ionic liquids. *Phys Chem Chem Phys* 12:1941–1947
- Zhao J, Dong C-C, Li C-X, Meng H, Wang Z-H (2006) Isobaric vapor-liquid equilibria for ethanol-water system containing different ionic liquids at atmospheric pressure. *Fluid Phase Equilib* 242:147–153. <https://doi.org/10.1016/j.fluid.2006.01.023>

Publisher's Note Springer Nature remains neutral with regard to jurisdictional claims in published maps and institutional affiliations.